

Strained graphene: tight-binding and density functional calculations

R. M. Ribeiro¹, Vitor M. Pereira², N. M. R. Peres¹, P. R. Briddon³, and A. H. Castro Neto²

¹Department of Physics and Center of Physics, University of Minho, Campus de Gualtar, 4710-057 Braga, Portugal,

E-mail: ricardo@fisica.uminho.pt, peres@fisica.uminho.pt

²Department of Physics, Boston University, 590 Commonwealth Avenue, Boston, MA 02215, USA,

E-mail: vpereira@bu.edu, neto@bu.edu

³School of Natural Sciences, University of Newcastle upon Tyne, Newcastle upon Tyne, NE1 7RU, United Kingdom

Abstract. We determine the band structure of graphene under strain using density functional calculations. The *ab-initio* band structure is then used to extract the best fit to the tight-binding hopping parameters used in a recent microscopic model of strained graphene. It is found that the hopping parameters may increase or decrease upon increasing strain, depending on the orientation of the applied stress. The fitted values are compared with an available parametrization for the dependence of the orbital overlap on the distance separating the two carbon atoms. It is also found that strain does not induce a gap in graphene, at least for deformations up to 10%.

New J. Phys.

PACS numbers: 81.05.Uw, 62.20.-x, 73.90.+f

1. Introduction

Graphene currently gathers an enormous amount of interest from many fronts. This stems, mostly, from it being a rare example of a system whose phenomenology spans a broad spectrum of fields. For example, graphene exhibits many uncommon transport signatures — as was established during the earliest experiments following its isolation [1, 2, 3] — and is an unexpectedly good conductor, despite being a strictly two-dimensional system. While graphene has many properties typical of *hard* condensed matter systems [4], it is simultaneously a soft membrane from a structural point of view [5, 6]. In fact, since reliable empirical potentials for carbon are generally available, and graphene isolation is now widely practiced, this system can become a new paradigm in membrane physics because both accurate microscopic modelling [7], and direct comparison with experiments are possible

The simple fact that graphene is an atomically-thick membrane has a high import for the interplay between its electronic and mechanical structures. One particular aspect of this interplay is the extent to which in-plane strain can modify graphene's electronic structure and, consequently, its transport characteristics. Strain-induced modifications of the electronic structure are usually negligible in conventional systems because of their three dimensional nature. Even in the thinnest films grown epitaxially on a mismatched substrate, strain is generally irrelevant for the bulk properties, insofar as it is rapidly and efficiently relieved from layer to layer above the substrate, either elastically, or by the intervention of defects [8]. Graphene, on the other hand, is a single-layer membrane, made out of sp^2 hybridized carbon bonds [9], which are the strongest in nature. If buckling is disregarded, strain cannot be relived in the third direction, nor in plane through the generation of defects, which are energetically costly. This tallies with recent experiments that place graphene as the strongest material ever measured, when it comes to the elastic response in the plane of the carbon atoms [10]. Graphene can sustain reversible (elastic) deformations of the order of 20%, as shown from *ab-initio* calculations [11] and recent experiments [12].

Despite these facts, the question of strain and its influence in the electronic structure of graphene has remained much unexplored until very recently. From the experimental point of view, important initial steps came from a series of investigations in the context of Raman spectroscopy [13]. Under in-plane strain the Raman peaks shift considerably, and can be split under anisotropic deformations. Their dependence with strain can be used to extract the Gruneissen parameters of graphene, which can be potentially quite usefull, for one can use a simple Raman measurement to *directly* identify and quantify strain profiles in graphene. Another seminal step was given by Kim and collaborators, who have investigated transport properties of graphene under strain, achieved by depositing samples on stretchable substrates [12].

From the theoretical front, a vital question is whether small and easily achievable strain can induce a bulk spectral gap in graphene's spectrum. If so, this would have enormous consequences in the context of a graphene device with tunable electronic structure. An early density functional theory calculation (DFT) [14] advanced that any arbitrarily small amount of uniaxial strain opens a gap in graphene's spectrum, whose magnitude varies non-monotonically with the amount of strain. These findings were apparently seconded by another *ab-initio* calculation [15], although there was strong disagreement between the magnitude of the gap among those two calculations, for the same amount of strain. Recently, however, Pereira and collaborators [17], using a tight-binding approach and treating deformations within linear continuum elasticity, challenged those conclusions. They showed that a spectral gap is achievable only for uniaxial deformations in excess of 20%, and that the effect strongly depends on the direction of the deformation with respect to the underlying lattice. These results are consistent with the investigations of Hasegawa *et al* which show that the gapless Dirac spectrum is robust with respect to arbitrary (and not exceedingly large) changes in the nearest-neighbor hoppings [18]. Recent developments from the *ab-initio* front [16, 19]

have shown results in agreement with the gappless scenario put forth in reference [17]. The apparent contradiction among different *ab-initio* calculations can be traced to the peculiarities of the electronic spectrum in graphene. In particular, the fact that, under strain, the Dirac point drifts away from the high-symmetry points of the lattice [17] was overlooked in the interpretation of the earliest results, and led to the erroneous conclusion that a gap seemed possible for any amount of strain.

Given that strain is now perceived as a new avenue of research in the physics of graphene, and given the importance of simple microscopic models that reliably describe the evolution of the electronic system under strain, we intend to further clarify these issues by pursuing two complimentary goals. We perform an *ab-initio* calculation of the band structure of graphene under uniaxial strain, for deformations up to 10%. The calculated bandstructure allows us to establish the absence of a spectral gap in the spectrum. Subsequently, we fit the tight-binding model used in reference [17] to the bandstructure obtained here *ab-initio*, in order to ascertain its range of validity, and to extract the model parameters. We conclude that the parameterization for the hopping integrals used in the cited reference is generally applicable in the entire range of deformations used in our study.

This paper is organized as follows. We start the next section by discussing the general features of strain in the honeycomb lattice, and the tight-binding parameterization that will be fit to our *ab-initio* bandstructure. In Sec. 3 we present the details of our DFT calculations, followed, in Sec. 4, by the procedure used here to study the electronic structure as a function of strain. The calculated bandstructures and their fitting to the tight-binding dispersion are shown and discussed in Sec. 5. In Sec. 6 we analyse the variation in the tight-binding hopping integrals, as fitted to the *ab-initio* bands, and compare their strain dependence with the analytical form proposed in reference [17].

2. General considerations on deformed graphene

In Fig. 1 we represent the unit cell of graphene, depicting the next nearest-neighbor vectors, δ_i ($i = 1, 2, 3$), and the hopping parameters, t_i . The primitive vectors, \mathbf{a} and \mathbf{b} , used in the DFT calculations are also shown. In this study we consider only two types of uniaxial strain: (i) along the x direction – corresponding to strain parallel to the zig-zag edge of the ribbon; (ii) along the y direction – corresponding to strain along the armchair edges of the ribbon. These correspond to two particular orientations of the more general uniaxial case discussed in Ref. [17], where an arbitrary orientation with respect to the lattice was considered. For small strain (appropriate for our study), the length of the vectors δ_i (in units of a_0) is given by [17]

$$\begin{aligned} |\delta_1| = |\delta_3| &= 1 + \frac{3}{4}\varepsilon - \frac{1}{4}\varepsilon\sigma, & |\delta_2| &= 1 - \varepsilon\sigma \\ |\delta_1| = |\delta_3| &= 1 + \frac{1}{4}\varepsilon - \frac{3}{4}\varepsilon\sigma, & |\delta_2| &= 1 + \varepsilon, \end{aligned} \quad (1)$$

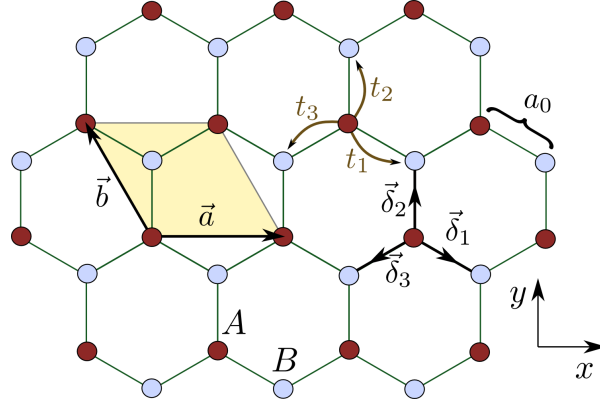


Figure 1. (Color online) Illustration of the honeycomb lattice with the A and B sublattices, the lattice vectors δ_i ($i = 1, 2, 3$), and the hopping parameters t_1 , t_2 and t_3 . The abscissas are along the zig-zag edge (horizontally in the figure). Also shown are the primitive vectors \mathbf{a} and \mathbf{b} used in the DFT calculation, and a_0 is the equilibrium carbon-carbon distance.

for zig-zag and armchair deformations, respectively. In our notation, ε represents the longitudinal strain and $\sigma = 0.165$ is the Poisson ratio, as measured for graphite [20], or $\sigma = 0.10 - 0.14$ for graphene as calculated in Ref. [19]. It is clear from Eq. (1) that both t_1 and t_3 will change upon stress by the same value, since the corresponding change in δ_1 and δ_3 is the same. In Ref. [17] it was found that:

- (i) For stress along the zig-zag edge, t_1 and t_3 decrease and t_2 increase upon increasing strain.
- (ii) For stress along the armchair edge, all t_i decrease, with t_2 being smaller than t_1 and t_3 .

These findings result from a combination of Eq. (1) with a parametrization for the change of the hopping parameters with the bond length given by [21]

$$V_{pp\pi} = t_0 e^{-\beta_i(l/a_0-1)}, \quad (2)$$

where t_0 is the hopping integral in free-standing graphene, l the bond length, and β_i a number of order $\beta_i \sim 3$. One of our goals is to verify to which extent this parametrization (2) is valid, starting from a full DFT calculation of graphene's bands under stress. With that purpose, we shall compare quantitatively the above parametrization for the variation of t_i with the values of t_i obtained from adjusting the tight-binding and DFT bands. For our DFT calculations it is convenient to write the primitive vectors of the unit cell as (see Fig. 1):

$$\mathbf{a} = a \mathbf{e}_x, \quad (3)$$

$$\mathbf{b} = -\frac{a}{2} \mathbf{e}_x + \frac{\sqrt{3}}{2} a \mathbf{e}_y, \quad (4)$$

The parameter a was varied when stress was applied along the x axis, and likewise for b , when stress is applied along the y direction.

3. Details of the DFT calculations

In our study of the spectrum of graphene under stress, density functional (DFT) calculations were performed with an *ab-initio* spin-density functional code (AIMPRO)[22], along with the local density approximation (LDA).

The Brillouin-zone (BZ) was sampled for integrations according to the scheme proposed by Monkhorst-Pack[23]. A grid of $12 \times 12 \times 1$ \mathbf{k} -points was generated and folded according to the symmetry of the BZ. An increase in the number of points did not result in a significant total energy change. However, a careful choice of the sampled \mathbf{k} -points is necessary in this study (see more below).

We use pseudo-potentials to describe the ion cores. Lower states (core states) are accounted for by using the dual-space separable pseudo-potentials by Hartwigsen, Goedecker, and Hutter[24]. The valence states are expanded over a set of s -, p -, and d -like Cartesian-Gaussian Bloch atom-centered functions, and the states are filled according to the Fermi-Dirac distribution using a value of $k_B T = 0.01$ eV, a procedure known to accelerate the convergence of the calculations. Kohn-Sham states are expressed as linear combinations of these basis functions, which were optimized for graphite.

Graphene was modeled in a slab geometry by including a vacuum region in a unit cell containing 2 carbon atoms. In the normal direction (z -direction), the vacuum separating repeating slabs has more than 30 Å ($c = 31.75$ Å). The size of the cell in the z -direction was optimized to make sure there was no interaction between repeating slabs. The size of the unit cell in the plane direction was optimized, and the lattice parameter after relaxation is $a = 2.4426$ Å. The tolerance for stopping structural optimization was 10^{-6} Ha. The tolerance for self-consistency was 10^{-6} Ha.

4. Bandstructure calculations under strain

Our calculations implement the deformation of the lattice along the following steps: the unit cell of graphene was first strained in the x direction and no relaxation was first allowed in the y direction, which is at first sight a reasonable approximation if the strain is small (this hypothesis is confirmed by the DFT calculations). This is validated by the small Poisson ratio for graphene, $\sigma \sim 0.10 - 0.14$, calculated in Ref. [19] for much larger strains. Latter, we have allowed the lattice to relax along the y axis, probing the energy landscape as a function of different bond lengths along y thus locating in this way the energy minimum of the relaxed lattice. The reasons for studying both the relaxed and unrelaxed lattice are given below. This allowed us to extract a Poisson ratio of $\sigma \sim 0.13 - 0.15$, in agreement with the calculations of Ref. [19]. The band structure of strained graphene was then calculated using DFT, for a fixed value of ϵ . The resulting DFT valence band around the \mathbf{K} -point was subsequently used to find the best values of t_i that fit the tight-binding bandstructure. Our choice of the valence band to fit the hopping parameters is motivated by the documented lack of accuracy of DFT in describing empty states. In the fitting procedure the bands were cut-off at 0.2

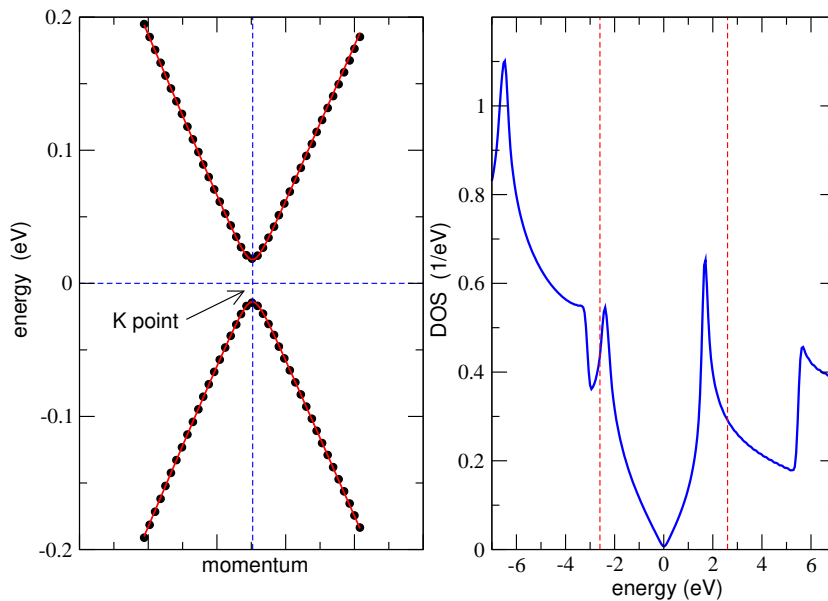


Figure 2. (Color online) Fitting of the DFT data (circles) to the tight-binding expression in Eq. (5) (solid line), for 1% strain (deformation along the x -direction). The fit is performed around the \mathbf{K} point in the BZ, and along the $\Gamma - \mathbf{K}$ direction. Note, however, that under strain the bands do not touch at the \mathbf{K} point anymore [17]. The system remains gapless, as can be seen on the right panel, where the density of states (DOS), as computed from DFT data for the same strain as in the left panel, is given. Also depicted in the right panel are the positions of the two Van Hove singularities in unstrained graphene (dashed lines).

eV, well inside the validity of the Dirac cone approximation for unstrained graphene. A fit for the values of t_i valid over the full energy range of the DFT graphene bands was found to be unsatisfactory using the simple Eq. (5). This is not surprising because Eq. (5) neglects details like the overlap factors of the orbitals, and other details discussed in Ref. [25]. In addition, the expression used for the tight-binding energy includes only hopping to the first neighbors, albeit with different values for the parameters t_1 , t_2 and t_3 [4]:

$$E = \pm |t_2 + t_3 e^{-i\mathbf{k}\cdot(\mathbf{a}+\mathbf{b})} + t_1 e^{-i\mathbf{k}\cdot\mathbf{b}}|. \quad (5)$$

If the lattice is strained only along the two chosen directions – x and y –, symmetry imposes that $t_3 = t_1$. The above procedure was then repeated for stress along the armchair direction.

5. DFT versus tight-binding

Figure 2 presents a fitting of Eq. (5) to the DFT results (points), together with the fitting (solid line) of the tight-binding Eq. (5). The fit of the numerical data to Eq. (5) was done for momenta around the \mathbf{K} point for all the values of strain. As can be seen in Fig. 2, for finite strain the touching of the valence and conducting bands does not happen at the \mathbf{K} point. This was shown explicitly in Ref. [17] and, as a result, any

plot of the bandstructure in the close vicinity of \mathbf{K} will inevitably show a fictitious gap. In reality the system remains gapless, as can be seen from the DFT density of states plotted in Fig. 2.

To fit the tight-binding dispersion we used twenty LDA points from each side of the \mathbf{K} point in the direction $\Gamma-\mathbf{K}$. As mentioned earlier, the fit was done only for the valence band, although Fig. 2 also shows the DFT data for the conduction band together with the tight-binding spectrum using the values of t_i from the fit to the valence band. The agreement is excellent. The 41 momentum points used for the fitting span a reciprocal length in momentum space of the order of 0.08 rad/bohr. A few notes are worth to be cast here. As strain is induced in graphene, the hexagonal symmetry is lost and the \mathbf{K} points do not retain their original position in the Brillouin zone. As an example, one of those symmetry points lies at the position given by the general expression:

$$\mathbf{K} = \left(\frac{c_{1y} c_{2x}^2 + c_{2y}^2 - c_{1x} c_{2x} - c_{1y} c_{2y}}{2 c_{1y} c_{2x} - c_{1x} c_{2y}} + \frac{c_{1x}}{2}, \right. \\ \left. - \frac{c_{1x} c_{2x}^2 + c_{2y}^2 - c_{1x} c_{2x} - c_{1y} c_{2y}}{2 c_{1y} c_{2x} - c_{1x} c_{2y}} + \frac{c_{1y}}{2} \right), \quad (6)$$

where

$$\mathbf{c}_1 = (c_{1x}, c_{1y}), \quad (7)$$

$$\mathbf{c}_2 = (c_{2x}, c_{2y}) \quad (8)$$

are the primitive vectors of the Brillouin zone, associated with the distorted unit cell (see Fig. 1). We have calculated the coordinates of the \mathbf{K} point for each value of the strain, and verified that the valence and conduction bands do not touch each other at this point. As found previously in [17] using a tight-binding approach, the \mathbf{K} point and the point in momentum space where the valence and conduction bands touch do not coincide. Our calculations show no gap opening in graphene, which agrees with the calculations of the cited reference, and also the DFT calculations of Ref. [19].

This point is indeed crucial for the discussion of the bandstructure under strain, since computing the spectrum around the \mathbf{K} point only may lead to the erroneous conclusion that strain opens a spectral gap [15], a fact not supported by a more detailed analysis [16, 19], and our current results. DFT methods, inevitably use a finite grid of momentum values over the Brillouin zone, which are used to sample the spectrum and the corresponding density of states. Using a too coarse sampling of the Brillouin zone is most likely bound to miss the precise momenta at which the valence and conduction bands touch. This would produce a density of states featuring an artificial non-existing gap, a consequence of an aliasing effect [15].

6. Tight-binding hopping parameterization

Figure 3 shows the variation of the hopping parameters as graphene endures stress along the zig-zag direction (upper panel). We have strained graphene's unit cell up to 10%, although experiments seem to indicate that the material can support reversible

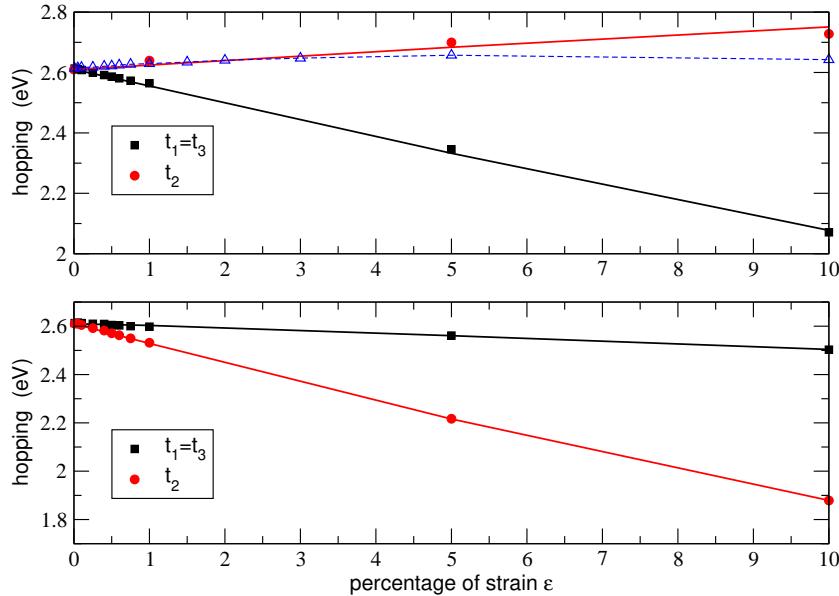


Figure 3. (Color online) Variation of hopping parameters, $t_1 = t_3$ and t_2 , as function of the strain ϵ determined from fitting Eq. (5) to the DFT valence band (points). The upper panel shows the case where the lattice is deformed along the zig-zag direction, while the lower panel refers to strain along the armchair direction. The solid lines represent the hopping computed using Eqs. (1) and (2) and the parametrization given in Table 6. The dashed line with triangles in the upper panel is the value of t_2 when the length of the corresponding bond is kept constant. The maximum amount of strain was 10%. The error bars are of the size of the points.

strains up to 20% [26]. The hopping parameter t_2 is perpendicular to this direction, and according to Eqs. (1) should have, in this case, a small variation due to the small value of the Poisson coefficient. Consequently, we have studied two cases for stress along the zig-zag direction: (i) keeping constant the bond distance associated with t_2 ; (ii) allowing this distance to vary, such that the energy of the strained lattice is minimum. The study (i) allow us to discuss whether the change in t_2 is only due to the bonding length modification or is also controlled by the redistribution of the electronic density around the carbon atoms. It is worth noticing that, according to the simple tight binding description of Eqs. (1) and (2), the change in the value of t_2 is due to the modification of the bond length alone, a result not observed in our DFT calculations, where t_2 varies with strain, even under the approximation of keeping the corresponding bond length constant (the variation of t_2 is, nevertheless, very small). Additionally, as graphene is strained along the zig-zag direction the hopping parameters t_1 and t_3 decrease, certainly due to the change of the bond length associated with these parameters. The overall results can be understood as follows: strain along the zig-zag direction increases the bond length along t_1 and t_3 directions and reduces the electronic density along these same bonds, additionally it increases the electronic density on the bond length associated with t_2 , even if no deformation is allowed for this bond. Consequently, t_1 and t_3 are reduced and t_2 increases slightly. This redistribution of electronic density among the

Stress	t_i	β_i
x -direction	$t_1 = t_3$	3.15
	t_2	4.0
y -direction	$t_1 = t_3$	2.6
	t_2	3.3

Table 1. Results for the parameter β_i in Eq. (2) for stress along the zig-zag (x -direction) and armchair (y -direction) directions, both considered in the text.

several bonds is effectively included in the tight binding description by allowing a change of all bond lengths, but this is not strictly necessary to observe the effect. We are then forced to conclude that the change in t_2 stems from a combination of the two effects: electronic density redistribution among the bonds and change in the bond length. This is in line with the fact that the relative orientation of the orbitals is also affected by the deformation and the resulting re-hybridization alone contributes to a modification of the effective hopping, even if the bond length remains unmodified. It is worth noticing that the values of t_2 for the relaxed and unrelaxed lattice are essentially the same for strain up to 3%, as seen in the upper panel of Fig. 2. The points for strains below 1% were obtained without relaxation in the direction perpendicular to the strain. The agreement of these points to the parametrization confirms our assumption that the relaxation is not important for small values of strain.

The situation is different for strain applied along the armchair direction (see lower panel of Fig. 3), because in this case all three bonds are deformed, up to first order in ε without any contribution from the Poisson coefficient, as can be seen from Eq. (1). Since the bond associated with t_2 decreases considerably more than the other two, this hopping decreases faster upon strain, an effect seen in Fig. 3.

In either the zig-zag or armchair cases, the bandstructure in the neighborhood of the neutrality point is seen to be well described by the parametrization used in the tight-binding analysis of Ref. [17], and given by Eq. (2). This fact is documented by the agreement between the solid lines and points in both panels of Fig. 3. In Table 1 we present the values of the parameter β_i [Eq. (2)] associated with each bond, extracted for the different cases studied here.

7. Conclusions

We have calculated the bandstructure of graphene under uniaxial strain *ab-initio*, within the LDA approximation. The spectrum remains gapless for all strain configurations studied, and up to the maximum value of longitudinal deformation (10%) used in our calculations, tallying with recent similar investigations [16, 19]. The *ab-initio* bandstructures were used to fit a tight-binding parametrization of the dispersion, from where we extracted the effective nearest-neighbor hopping parameters, and their dependence with the magnitude of deformation. As is generally known, hopping

parameters calculated using DFT are lower than the experimental ones, which is also seen in our calculations that show an unstrained hopping of 2.6 eV. Nevertheless DFT is accurate when calculating energy differences, and thus we believe that the slopes β_i of the hopping parameters calculated above should be close to the experimental values. Moreover, the behavior seen for the dependence of t_i on ε follows rather well the trend given by Eq. (2). We expect that the results found for β_i can be extrapolated to large values of ε with a certain degree of confidence.

Acknowledgments

We wish to acknowledge the support of the Fundação para a Ciência e a Tecnologia (FCT) under the SeARCH (Services and Advanced Research Computing with HTC/HPC clusters) project, funded by FCT under contract CONC-REEQ/443/2005. VMP and NMRP are supported by FCT via grant reference PTDC/FIS/64404/2006. AHCN acknowledges the partial support of the U.S. Department of Energy under the grant DE-FG02-08ER46512.

References

- [1] K. S. Novoselov *et al* , Science **306**, 666 (2004).
- [2] K. S. Novoselov *et al* , Nature **438**, 107 (2005).
- [3] M. I. Katsnelson, K. S. Novoselov and A. K. Geim, Nature Physics **2**, 620 (2006).
- [4] A. H. Castro Neto, F. Guinea, N. M. Peres, K. S. Novoselov, and A. K. Geim, Rev. Mod. Phys. **81**, 109 (2009).
- [5] Jannik C. Meyer *et al* , Nature **446**, 60 (2007).
- [6] Eun-Ah Kim and A. H. Castro Neto, Eur. Phys. Lett. **84**, 57007 (2008).
- [7] A. Fasolino, J. H. Los and M. I. Katsnelson, Nature Materials **6**, 858 (2007).
- [8] J.W. Matthews and A.E. Blakeslee, J. Cryst. Growth **27**, 118 (1974).
- [9] N. M. R. Peres, *Graphene: new physics in two dimensions*, **40** issue 3, Europhysics News (2009).
- [10] Changgu Lee, Xiaoding Wei, Jeffrey W. Kysar, and James Hone, Science **321**, 385 (2008).
- [11] F. Liu, P. Ming, and Ju Li, Phys. Rev. B **76**, 064120 (2007).
- [12] Keun S Kim *et al* , Nature **457**, 706 (2009).
- [13] Z. H. Ni *et al* , ACS Nano **2**, 2301 (2008); Z. H. Ni *et al* , Phys. Rev. B **77**, (2008); T. Yu *et al* , J. Phys. Chem. C **112**, 12602 (2008); J. A. Robinson *et al* , Nano Lett. **9**, 964 (2009); S. Berciaud *et al* , Nano Lett. **9**, 346 (2009); T. M. G. Mohiuddin *et al* , arXiv:0812.1538; M. Huang *et al* , arXiv:0812.2258.
- [14] G. Gui, J. Li, and J. Zhong, Phys. Rev. B **78**, 075435 (2008).
- [15] Z. Ni *et al* , ACS Nano **2**, 2301 (2008).
- [16] Z. Ni *et al* , ACS Nano **3**, 483 (2009).
- [17] Vitor M. Pereira, A. H. Castro Neto, and N. M. R. Peres, arXiv:0811.4396.
- [18] Y. Hasegawa, R. Konno, H. Nakano, and M. Kohmoto, Phys. Rev. B **74**, 033413 (2006).
- [19] M. Farjam and H. Rafii-Tabar arXiv:0903.1702.
- [20] L. Blakslee, D. G. Proctor, E. J. Seldin, G. B. Stence, and T. Wen, J. Appl. Phys. **41**, 3373 (1970).
- [21] D. A. Papaconstantopoulos, M. J. Mehl, S. C. Erwin, and M. R. Pederson, in Tight-Binding Approach to Computational Materials Science, edited by P. Turchi, A. Gonis, and L. Colombo (Materials Research Society, Pittsburgh, 1998), p. 221.
- [22] M. J. Rayson and P. R. Briddon Rapid iterative method for electronic-structure eigenproblems using localised basis functions Comput. Phys. Commun. **178** (2008) 128-134.

- [23] H. J. Monkhorstand J. D. Pack, Phys. Rev. B **13**, 5188 (1976).
- [24] C. Hartwigsen, S. Goedecker, and J. Hutter, Phys. Rev. B **58**, 3641(1998).
- [25] S. Reich, J. Maultzsch, C. Thomsen, and P. Ordejón, Phys. Rev. B **66**, 035412 (2002).
- [26] F. Liu, P. Ming, and J. Li, Phys. Rev. B **76**, 064120 (2007)